Cretaceous Research 147 (2023) 105507

Contents lists available at ScienceDirect

Cretaceous Research

journal homepage: www.elsevier.com/locate/CretRes

Rudist reef structure: Insights from orientation of hippuritids at l'Espà (Campanian, southern Pyrenees)

C. Boix [a], E. Vicens [b], V. Riera [c], O. Oms [b, *]

[a] Universidad de Alcalá, Departamento de Geología, Geografía y Medio Ambiente, Campus Científico Tecnológico, 28802 Alcalá de Henares, Spain
[b] Universitat Autònoma de Barcelona, Facultat de Ciències, Departament de Geologia, 08193 Bellaterra, Spain
[c] Centro de Estudios y Experimentación de Obras Públicas, 28014 Madrid, Spain

ARTICLE INFO

Article history:
Received 4 October 2022
Received in revised form
9 February 2023
Accepted in revised form 12 February 2023
Available online 17 February 2023

Keywords:
Hippuritids
Carbonates
Microfacies
Paleoecology
Foreland basin

ABSTRACT

Rudist were common Mesozoic reef builders, but rare examples exist to evaluate reef structure. The l'Espà locality (southern Pyrenees) is approached to study rudist reef structure by a quantitative assessment of the individuals' position (growing *vs* reworked) and its sedimentary context. This late Campanian reef is exposed along some 20 × 6 m outcrop. Builders are mainly *Hippurites radiosus*, although other rudists, such as *Hippuritella lapeirousei*, *Hippuritella* sp. and *Mitrocaprina* sp. are also present together with corals. The orientation of 325 specimens of mainly *H. radiosus* was plotted in stereographic and cartesian projections. Orientations and microfacies permit to differentiate 5 vertically stacked intervals (settings) along the outcrop: (1) Distal reef setting (reef-talus slope), with rudists reworked as large bunches of grouped specimens, with scarce erosion and preserving both valves articulated; (2) Halfway distal-proximal reef setting (close cluster reef), with abundant reworked, isolated, and flat-lying specimens. In this zone, endo-epibiont colonization on rudist shells is common, together with the presence of large (up to 1 m) branching and massive corals; (3) Proximal reef setting (frame/close cluster reef), where specimens are in life position; (4) A proximal back reef unit (spaced cluster reef) with few highly reworked specimens; (5) Distal back reef setting (very spaced cluster reef), with hardly any rudist fragments. This succession provides a reef tract model resembling that of most coral reefs and differs from smaller rudist reefs. The structure of the studied reef is well preserved as a result of high accommodation space related to thrust emplacement.

1. Introduction

The understanding of reef structure from the geological record appears limited when dealing with extinct reef builders such as rudists. The role of these reefs is not only important in the understanding of marine Mesozoic carbonate factories and ecosystems, but it is also a key point to understanding the geometry of the still-producing giant oil fields (Sadooni, 2005; Yose et al., 2006; Yamanaka et al., 2020). The issue of whether rudists formed rigid reef frameworks (Schumann, 1995) or were bafflers forming baffle-stones in a micritic matrix (Özer and Benyoucef, 2021) is here addressed by means of a well-documented and quantified study case. Several works dealing with the structure of rudist reefs are generally limited by the available information (outcrops size, limited core data, number of specimens, diagenesis and dissolution, etc.). The rudist reef record of the Iberian Peninsula is an exception, since several well-exposed examples are found for different ages which contain large amounts of specimens. Other than taxonomical and succession studies, several works included stratigraphic architecture (Sanders and Pons, 2001), the occurrence of the corals/rudists assemblage and interactions (Gili et al., 1995; Götz, 2003), the growth fabric (Skelton et al., 1995) and a single-bed quantification of rudists orientation (Vilardell and Gili, 2003). These works did not focus on the succession of accurate space orientation of specimens, which is here addressed to understand rudist reef structure. Finally, it will be evaluated if the obtained structure is similar to that of other kinds of reefs as well as the relationship between reef structure and environment (Gil et al., 2009) or rudist growth patterns.

The l'Espà reef was first referred to by Moeri (1977). Systematic studies by Vicens (1992), reported the elongated rudist *Hippurites*

* Corresponding author.
E-mail addresses: carme.boix@uah.es (C. Boix), enric.vicens@uab.cat (E. Vicens), Spain.violeta.riera@cedex.es (V. Riera), joseporiol.oms@uab.cat (O. Oms).

https://doi.org/10.1016/j.cretres.2023.105507

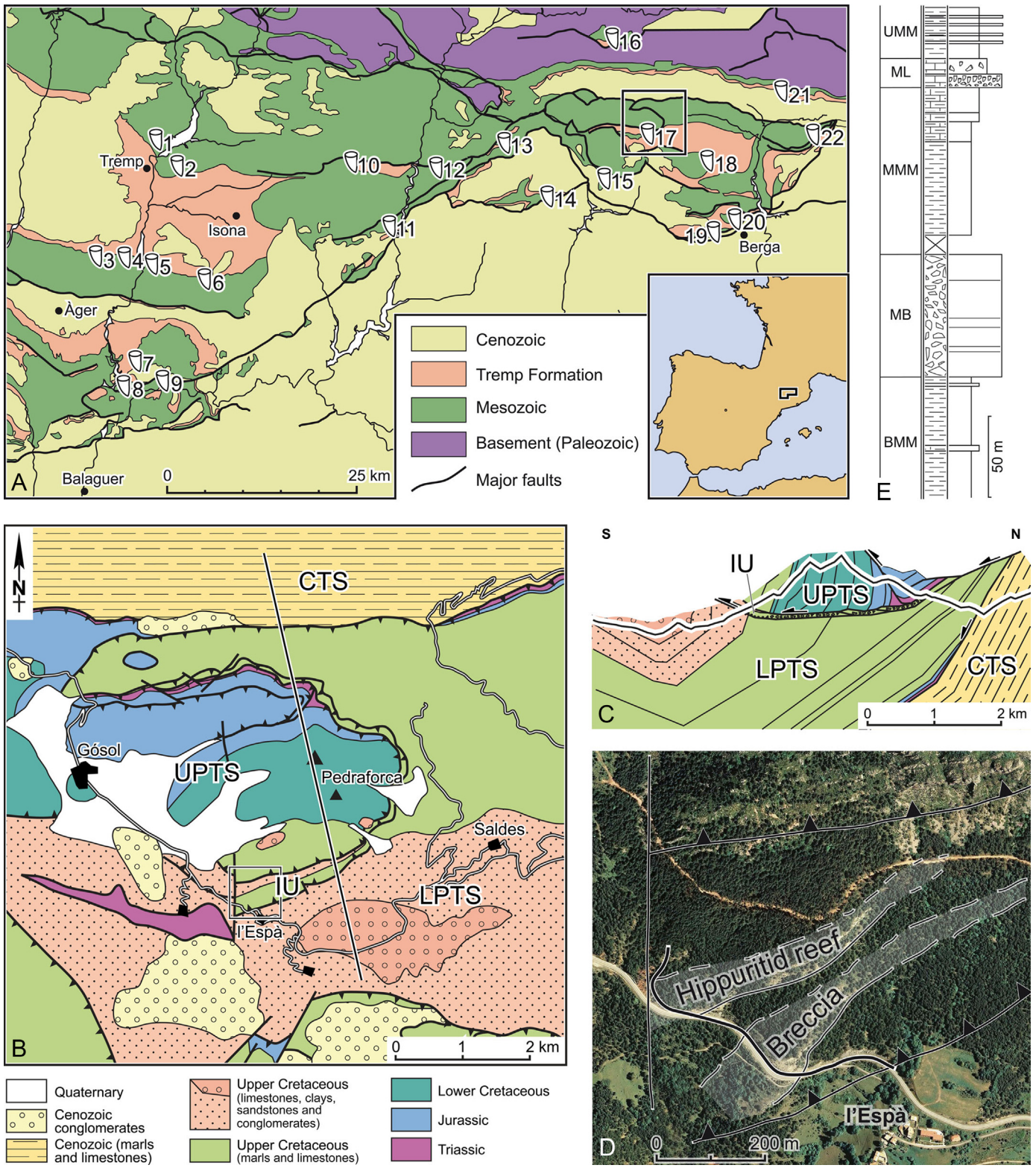

Fig. 1. A: Simplified geological map of the South-central and South-western Pyrenees (see geographic location in the frame of Iberia) with the indication of the localities with *Hippurites radiosus* (after Vicens, 1992; Vicens et al., 2004; Oms et al., 2016; Caus et al., 2016; Robles-Salcedo et al., 2013, 2018): (1) Homes Morts from Santa Engracia; (2) Sant Vicenç de Galliner; (3) Homes Morts from Moror; (4) Serrat Pedregós; (5) Terradets; (6) Hostal Roig: (7) La Massana o el Coscoll; (8) Penalta; (9) Alòs de Balaguer; (10) Sallent; (11) Peramola; (12) Canelles; (13) Ossera; (14) Coll de Jou; (15) Serra de Pratformiu; (16) El Querforadat; (17) L'Espà; (18) Pla de la Barraca, Torrent del Forat Negre or Tumí; (19) Cal Portet; (20) Vilaformiu; (21) Coll de Pal; (22) El Catllaràs. B: Detailed geological map (adapted from Martínez et al., 2001) of the Pedraforca mountain area and the l'Espà village. The cross-section in Fig. 1C and photomap in Fig. 1D are also indicated. Abbreviations: CTS: Cadí thrust sheet, LPTS: Lower Pedaforca thrust sheet, IU: Pedraforca Intermediate Unit. UPTS: Upper Pedraforca thrust sheet. C: Geological cross-section (see location in Fig. 1b) of the Pedraforca mountain area and location of the studied outcrop in the Pedraforca Intermediate Unit (abbreviations as in Fig. 1B). D: Photomap (see location in Fig. 1B) of the studied outcrop with the location of the general section (after Vicens, 1992). Image from http://icc.cat. E: Regional lithostratigraphic units (Vicens, 1992): BMM (basal marine marlstones), MB (marine breccia), UMM (upper marine marlstones), MMM (middle marine marlstones), ML (marine limestone), UMM (upper marine marlstones).

Fig. 2. Outcrops at l'Espà reef. A: Interval 1 (proximal reef slope) in lateral outcrop. B: transition from interval 1 to 2 (close cluster reef) in the main outcrop. C: 1-m-thick massive colonial coral in interval 3 in lateral outcrop, including a large coral block (separated by a dashed line). D: transition from interval 2 to 3 (close cluster reef to frame/close cluster reef) in lateral outcrop. E: transition from interval 2 to 3 in lateral outcrop from D. F: Interval 3 in the main outcrop. *Hippurites radiosus* are reworked in Fig. 2A–C, but in life position in upper 2E and whole 2F. Image 2B corresponds to the same outcrop in figure 4 of table 2 in Moeri (1977). The thin solid lines in 2B, 2D and 2E mark the mentioned transitions between intervals.

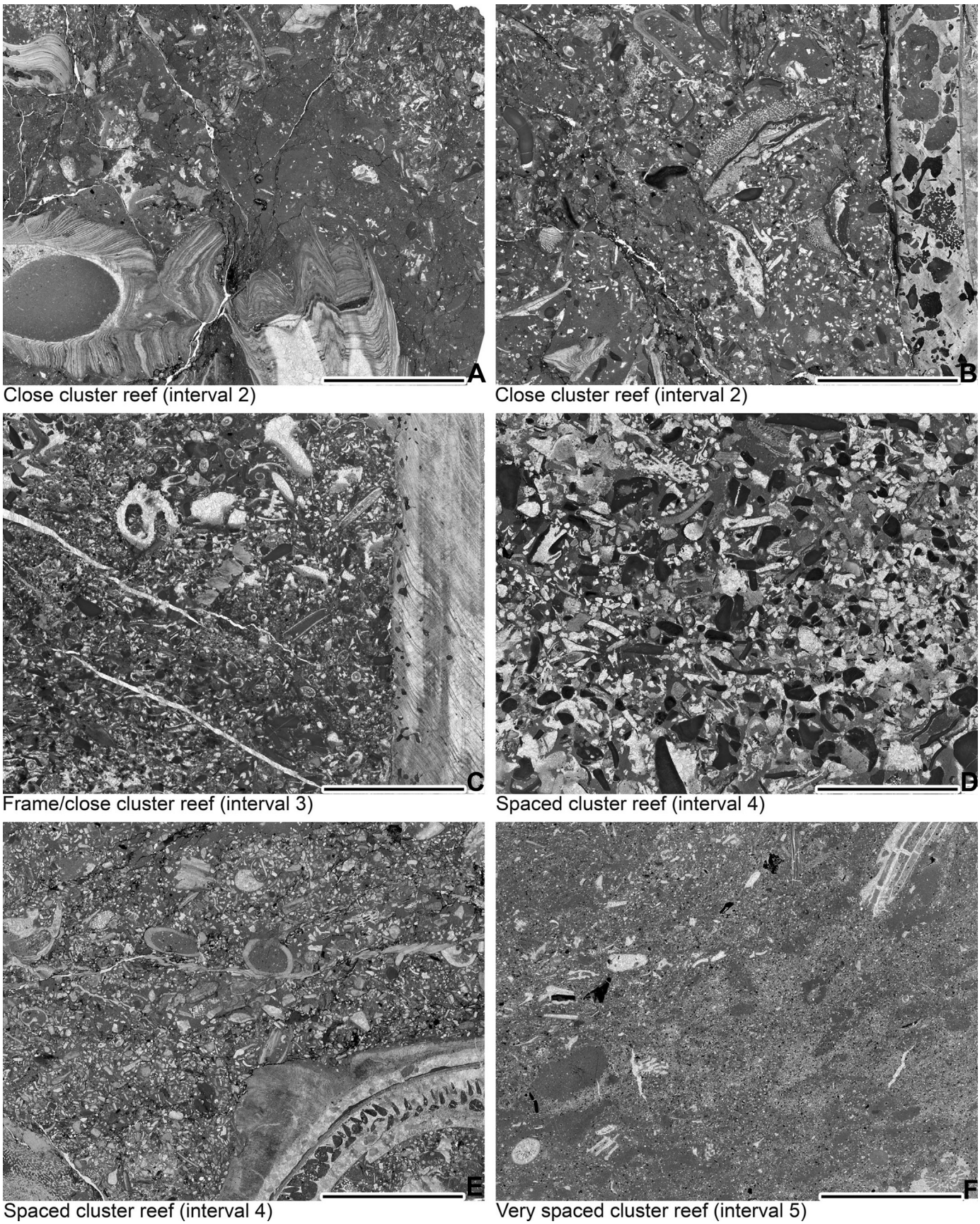

Fig. 3. Representative microfacies from the l'Espà reef. Interval 2 (A, B): Dominated by packstones and floatstones with a wacke-packstone texture matrix. Bivalve fragments (including rudists), echinoids, bryozoan, and calcareous red and green algae fragments are common. Interval 3 (C): Skeletal-rich packstone, with small benthic foraminífera, bivalve,

radiosus as the main component; although other rudists, such as *Hippuritella lapeirousei*, *Hippuritella* sp. and *Mitrocaprina* sp. are also present, but far less abundant. *H. radiosus* is a common species at the Late Cretaceous platforms of the western Pyrenees (Bilotte, 1985). *H. radiosus* is an hippuritid with a mean length of around 45 cm (although some specimens can be longer than 70 cm) and a width of 71.5 mm (width based on 263 measures at l'Espà). *Hippuritella* sp. is a relatively medium-sized hippuritid, with a length between 5 and 15 cm and a width of 34.3 mm (based on 9 measures). Radiolitids' length is relatively very small (less than 10 cm).

According to the rudists morphotype classification by Skelton and Gili (1991), *Hippurites radiosus* would be a cylindrical elevator, with vertical upward growth, with specimens displaying isolated growth to dense clusters of mutual cemented rudist. According to Mitchell (2002), it can be considered a cluster elevator.

The studied reef is located 500 m to the NW of the l'Espà village (see Fig. 1). The main studied section is found in a relatively large outcrop (up to 20 × 6 m) in the road cut between the villages of Saldes and Gósol (Barcelona and Lleida provinces, respectively). The extension of this reef can be tracked to the east for some 600 m in the forests of the southern slope of the Pedraforca massif (see Fig. 1D). The roadcut outcrop is the Point of Geological Interest with inventory number 146 (l'Espà- Saldes) of the regional administration (Martínez, 2000) and has been visited during several paleontological congresses (Vicens et al., 2011, 2014).

2. Geological setting

The studied reef is geologically located in the Pyrenean basin, which developed at the boundary between the European and Iberian plates. During the Cretaceous, this basin underwent two tectonic stages (see review in Muñoz et al., 2018). First, a distensive stage (post-rift) separating the two plates took place from the Lower Cretaceous to the Santonian. A second compressive (foreland) stage took place from the Santonian to the Maastrichtian, when the two plates collided. The evolution from one stage to the other took place by inversion tectonics (fault reactivation). Uplift in the compressive stages promoted important rudist reef-building both in local shoals and relatively extensive platforms. According to the genetic classification of Cenozoic carbonate platforms based on their basinal and tectonic settings (Bosence, 2005), the l'Espà reef belongs to the thrust-top platforms type.

The compressive stage continued in the Cenozoic until the Eocene, structuring cover units in several thrust sheets. In the South-Western Pyrenees, two main cover structural units are found: the Cadí and the Pedraforca thrust sheets. The latter is built up by the stacking of two main units known as the lower, and upper Pedraforca. Between these two units, a smaller one is found, which has been referred to as the Pedraforca Intermediate Unit (IU, Fig. 1B and C). The tectosedimentary role of this last unit has been studied for the Maastrichtian (Vergés and Martínez, 1988; Martínez et al., 2001; García Senz, 2002). The sedimentary succession of the Intermediate Unit (see Fig. 1E) is thicker than 250 m and is built up of 6 lithologic units, from base to top: basal marine marlstones, marine breccia (colluvium derived from the Early Cretaceous from the Upper Pedraforca thrust sheet), middle marine marlstones and marine limestones (being most of the succession here studied), and upper marine marlstones with fine-grained sandstones (being the upper part of the studied succession). In the roadcut, above these materials, the outcrops of the terrestrial/transitional Tremp Formation (marlstones, sands, and intraclast breccia) are found, containing fragments of the Maastrichtian oospecies *Megaloolitus siruguei* (Vila et al., 2011). Unfortunately, hardly any sedimentological or paleoecological data exist on the paleogeography affecting the rocks that build the Intermediate Unit, whose best locality for the study of rudists is l'Espà.

The late Campanian age for the l'Espà reef is constrained through the magnetostratigraphic age of the overlying continental strata (Oms et al., 2007) and by Pyrenean rudist zonation (Vicens, 1992; Vicens et al., 2004). This age is also confirmed by the 71 Ma isotopic dating of *Hippurites radiosus* platform (Caus et al., 2016) at 'Homes morts de Santa Engracia' (locality 1 in Fig. 1A).

3. Methods

Field methods included the acquisition of sedimentological and paleontological data. Sedimentological data comprised the logging of the lithological description, with special care on the description of the proportions and relationships between matrix and rudist shells. Twenty-seven rock samples were collected for general microfacies observations (see location in Fig. 4, right). Sampling avoided any significant damage to the outcrop.

Most of the paleontological data collection consisted of the measurement of the orientation of *Hippurites radiosus* specimens, the dominant species in the outcrop. The longitudinal striations of the elongated (right) valves were measured with a compass to determine the azimuth and dipping angle of each specimen (i.e, angular determination with the north and the horizontal plane, respectively). Special care was taken to determine if specimens were or were not overturned. This was easily determined when the small (left) valve or the apex could be observed. When the small valve or the apex were not visible, the longitudinal section was useful (i.e., the pattern of pillars and folds that are distinctive of this species). All measurable specimens were considered, i.e., the ones accessible both standing by the wall or using a ladder. Few geniculated specimens (as some examples in Fig. 2D and E) are found, but only rectilinear ones have been measured. Of particular importance was also the accurate measuring of bedding orientation at the l'Espà section. This allowed a further dipping correction of rudists' orientations. The observation of endo-epibionts affecting rudists plus the corals-rudists relationships were also carried out. The complete list of these measurements is available as online Supplementary material.

Laboratory work included the microfacies description of thin sections obtained from the samples and the plotting of rudists' orientations.To plot these orientations in a comprehensive 3D scheme, they were represented in a standard stereographic projection using Stereonet software (Allmendinger et al., 2012). This technique permits a visualization of the azimuth and dipping of all specimens as in the study by Negra et al. (2016). Additionally, a cartesian 2D display of inclination vs stratigraphic height was also designed to locate inclination data along with the stratigraphic log (Fig. 5). The studied thin sections are available and hosted at the repository board at room C2/324 (Geology Department, Universitat Autònoma de Barcelona) with the identification codes 'ES01' to 'ES15' and 'E00' to 'E11'.

4. Results

The lithological logging at the l'Espà reef and the relationship between matrix and rudist shells permitted the distinction of five

echinoid, green algae, and coral fragments. Minor presence of mm-scale bivalve and red-algae fragments. Interval 4 (D, E): Floatstones with a packstone matrix, with a common presence of bivalves, red and green algae, bryozoans, and small benthic foraminifera. Note the presence of encrusting algae and sponges on the largest skeletal allochems. Interval 5 (F): Packstone with fine-grained skeletal allochems, most of them affected by dissolution. Presence of bivalve, bryozoan, coral and echinoderm fragments, serpulids, ostracods, and small benthic foraminifera. The graphic scale is 1 cm. The muddy appearance of interval 1 matrix is not here included.

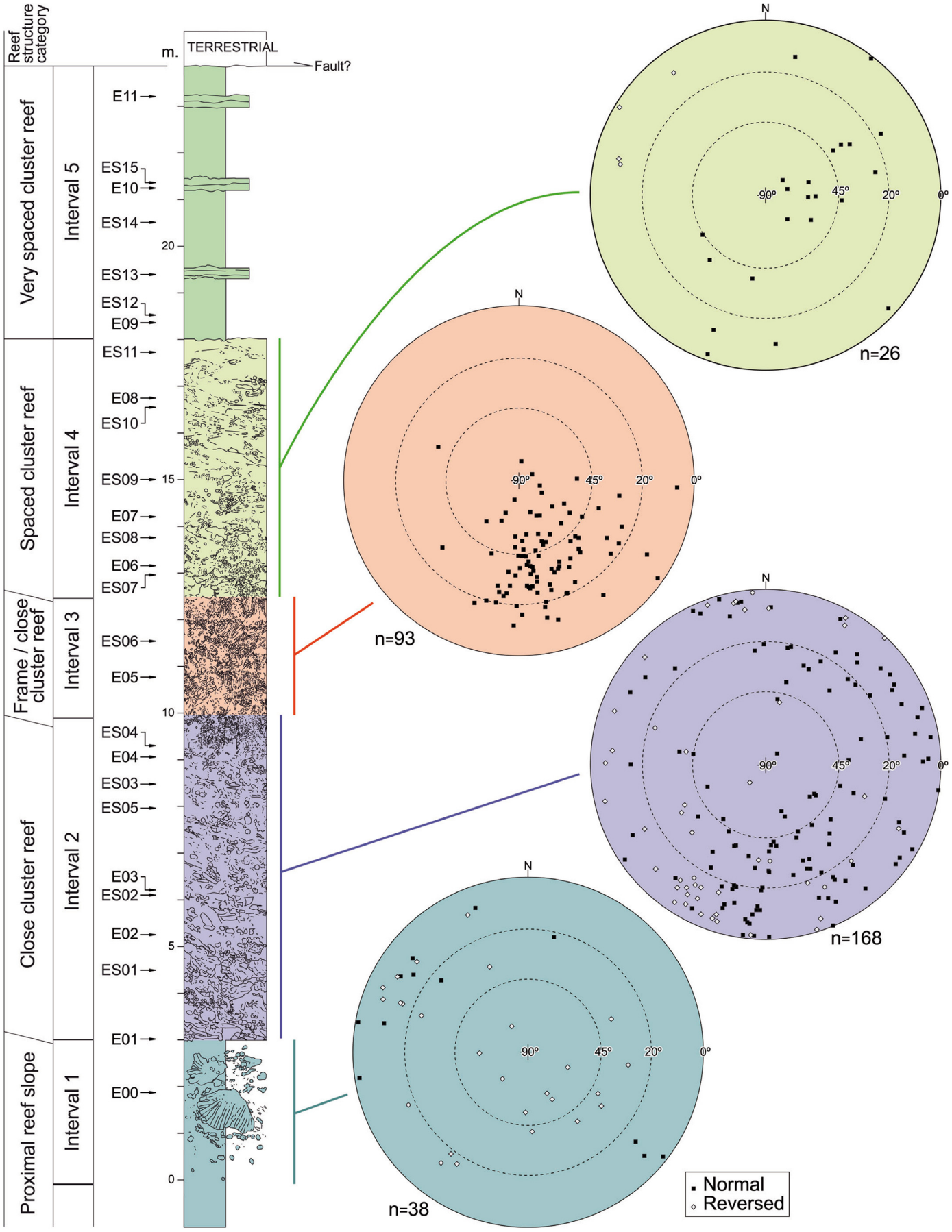
Reef structure category
Very spaced cluster reef
Spaced cluster reef
Frame / close cluster reef
Close cluster reef
Proximal reef slope
Interval 5
Interval 4
Interval 3
Interval 2
Interval 1
m.
TERRESTRIAL
Fault?
E11
ES15
E10
ES14
ES13
ES12
E09
ES11
E08
ES10
ES09
E07
ES08
E06
ES07
ES06
E05
ES04
E04
ES03
ES05
E03
ES02
E02
ES01
E01
E00
20
15
10
5
0
N
90°
45°
20°
0°
n=26
n=93
n=168
n=38
Normal
Reversed

main lithologic intervals (see Supplementary Figs. 1 and 3). As it will be later shown, each interval showed distinctive microfacies (Figs. 3 and 4).

Regarding rudists' orientations, 325 measures were obtained throughout intervals 1 and 4. After measuring all the available specimens, the amount of orientation data is large, and the spacing of data is narrow, except for interval 4. This exception is due to the forming processes (see later) rather than a sampling bias. Plots in Fig. 4 (right) and 5A contain all measured orientation data, which are split into the five descriptive units.

4.1. Interval 1

In the 3 measured meters of the first interval, 38 rudist orientations were measured. They display a random pattern with 26 reverse and 12 normally oriented specimens (see Figs. 4 and 5A and Supplementary Table 1). Declination and inclination values are quite scattered and only a slight dominance of reverse orientation can be observed in specimens of high-inclination angle. The percentage of marly matrix vs rudists is very high at the base of the interval (c. 90% of marlstones), while towards the top it decreases up to c. 30%, with the rudist shells being in contact. Rudist shells are parautochthonous, being both isolated specimens or large bunches (Figs. 2A and B). The preservation of the shells is excellent, with no evidence of dissolution and scarce erosion. Both valves are generally found articulated.

Microfacies determinations show an overall floatstone texture for interval 1, with centimetric skeletal allochem fragments and abundant, locally recrystallized micritic matrix, with argillaceous seams and incipient microstylolites. The skeletal assemblage is represented by cm-scale fragments of colonial corals and bivalves (including rudists) locally encrusted by serpulids. Within the matrix, scarce ostracods and bryozoan fragments, and rare presence of red algae fragments and miliolids (foraminifera) are also observed.

In this interval three rudists types are found (Fig. 5A): very rare *Mitrocaprina* sp., rare *Hippuritella* sp. and abundant *Hippurites radiosus*. Corals are very rare as well as endo-epibiont colonization. This last colonization is just rareat the uppermost part of the interval.

4.2. Interval 2

In the second interval (which is 7 m thick), the 168 available measurements show a non-random pattern compared to the previous interval 1 (see Figs. 4 and 5A). Despite declination values being rather scattered, rare high inclination values are observed in interval 2. One hundred and twenty specimens are in normal orientation, and 48 are in a reverse position. Shells are close to each other but not always in contact (see Fig. 2A). Rudists are not in a life position and are generally flat-lying (see Fig. 2B). It is remarkable that rudists' shells display scarce erosion and that they preserve both valves articulated. Important endo-epibiont colonization is typical from this interval. It occurs as borers (see Fig. 3B) or as encrusting organisms. Accessory reef builders are also typical of this interval, being both branching and massive colonial corals. Some of these massive corals may be up to 1 m thick (Fig. 3C).

Microfacies in interval 2 are diverse (see Fig. 3A and B). At the base of the interval, mudstones to locally peloid-rich wacke-packstones are present. Despite local dissolution (of matrix and allochems) and late calcite cement precipitation, the skeletal assemblage is poor in diversity, mostly represented by a minor presence of cm-scale fragments of rudists and colonial corals (recrystallized), ostracods, and a very rare presence of echinoid fragments and small benthic foraminifera (miliolids and biserial textulariids). Calcite-occluded microfractures and microstylolites are also present.

Microfacies from the middle and upper part of interval 2 display a large variety: from a wackestone texture with abundant micritic matrix, skeletal-rich floatstone with a micrite-poor packstone matrix, to fine-grained packstone with most of the micritic matrix being replaced by finely crystalline sparite. Some of the intraclasts have been recrystallized. Large, cm-scale bivalve and coral fragments are present (see Fig. 3A), displaying alterations such as borings and/or micritic coats (see Fig. 3B). Gastropod, red algae, codiacean and dasyclad fragments are common, with a minor presence of ostracods and small benthic foraminifera (miliolids, rotaliids, and small meandropsinids).

Four rudist types have been found in this interval: few *Mitrocaprina* sp. and *Hippuritella* sp., abundant *Hippurites radiosus* and very rare radiolitids. Few corals are observed and colonization by endo-epibionts is rarely observed, although it progressively decreases towards the top of the interval.

4.3. Interval 3

In the third interval, which is 3 m thick, all 93 measurements show normal orientations and depict a completely different pattern (Figs. 4 and 5A). Not a single specimen in a reverse position is detected, and a general grouping of values is observed. This grouping depicts a general S/SE leaning of rudists specimens. Interval 3 is entirely built up of in-place shells, which are in contact (see Fig. 3E and F). The absence of corals as reef builders is notable.

The dominant microfacies is a packstone texture with a micritic matrix replaced by very fine crystalline calcite. Some of the bioclasts have also been replaced by sparite. Most of the allochems are fine and very fine-grained, with a minor presence of mm-scale grains (red algae and bivalve fragments, including rudists) (see Fig. 3C). The rest of the skeletal assemblage comprises echinoid fragments, foraminifera (small miliolids, textulariids and rotaliids), and a scarce presence of ostracods, coral and green algae fragments. Longitudinal and parallel fractures are occluded by calcite cement.

This is the interval with the lowest biodiversity in terms of the selected taxa and has neither corals nor endo-epibiont colonization. *Hippurites radiosus* is abundant, only few *Hippuritella* sp. are found and *Mitrocaprina* sp. is very rare.

4.4. Interval 4

In interval 4, which is 5.5 m thick, only 26 orientations could be obtained, 4 showing reverse orientations and 22 showing normal ones (see Figs. 4 and 5A). This small amount of data is attributable to three factors: the inaccessibility of the outcrop (high in the roadcut), the recent weathering of the rock (barely unaltered), and a limited number of measurable specimens. Despite the small amount of data, a dominant NE–SW trend is observed.

The microfacies study of the lower and middle part of interval 4 shows that the sediment between the rudist shells has an overall floatstone texture, with a packstone texture matrix. The largest (few mm to cm-scale) skeletal components are fragments of

Fig. 4. The l'Espà rudist reef section. Left: several features and main units. Center: lithologic succession. Right: stereoplots (see Fig. Suppl. 2) of rudists orientations. Black squares represent normal dipping specimens, i.e., those with the apex pointing downwards (or small valve upwards). Conversely, white diamonds are reversed, i.e., with the apex pointing upwards (or small valve pointing downwards).

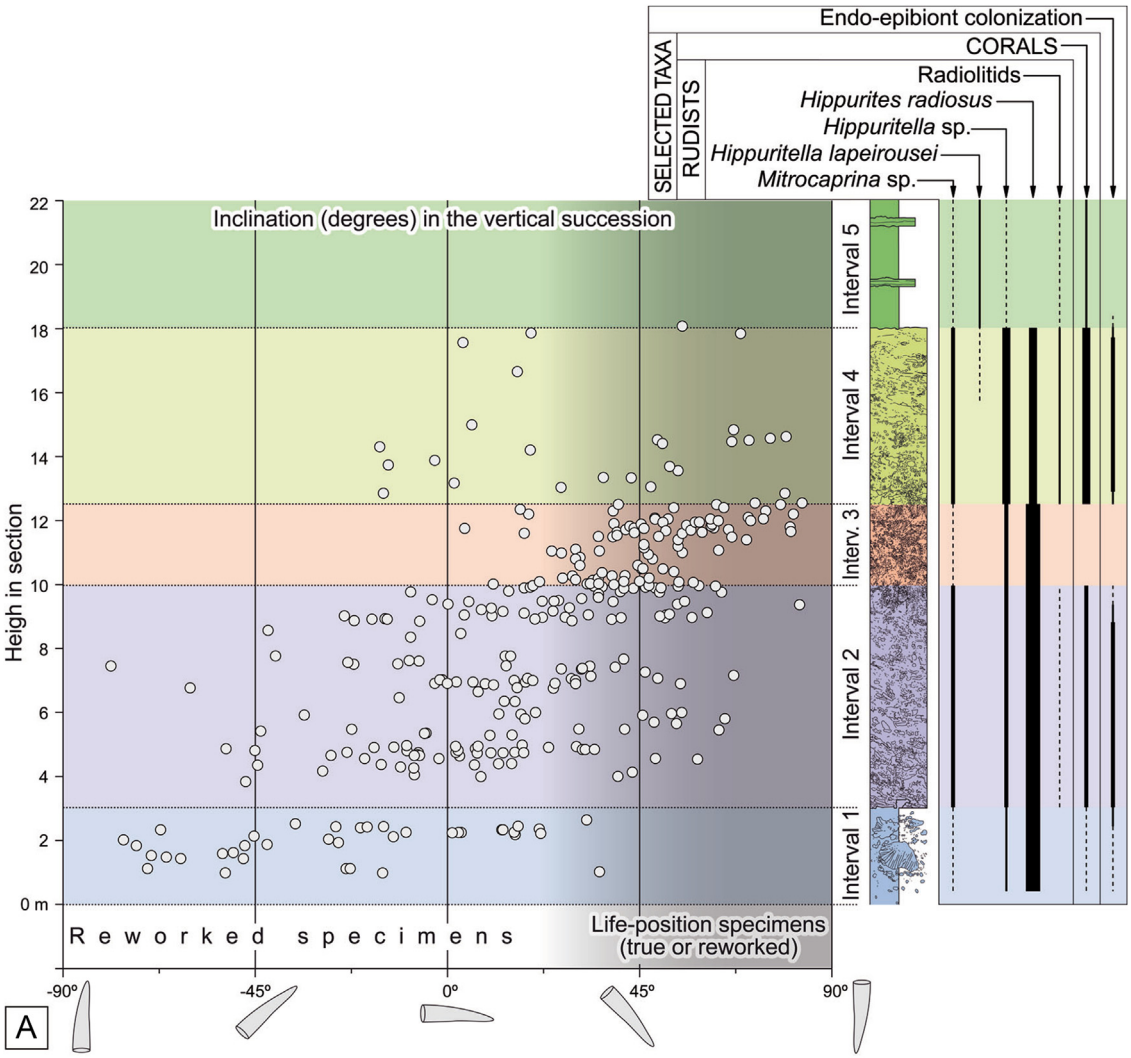
Endo-epibiont colonization
CORALS
Radiolitids
Hippurites radiosus
Hippuritella sp.
Hippuritella lapeirousei
Mitrocaprina sp.
SELECTED TAXA
RUDISTS
Inclination (degrees) in the vertical succession
Heigh in section
22
20
18
16
14
12
10
8
6
4
2
0 m
Interval 5
Interval 4
Interv. 3
Interval 2
Interval 1
Reworked specimens
Life-position specimens (true or reworked)
-90º
-45º
0º
45º
90º
A

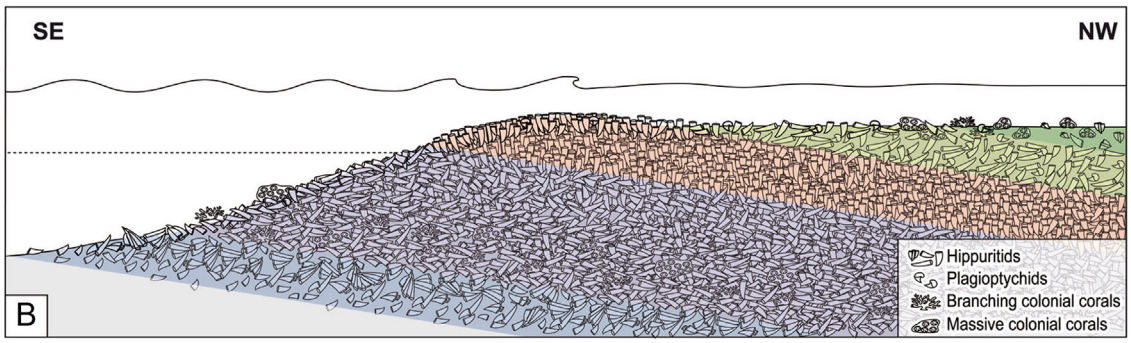
SE
NW
Hippuritids
Plagioptychids
Branching colonial corals
Massive colonial corals
B

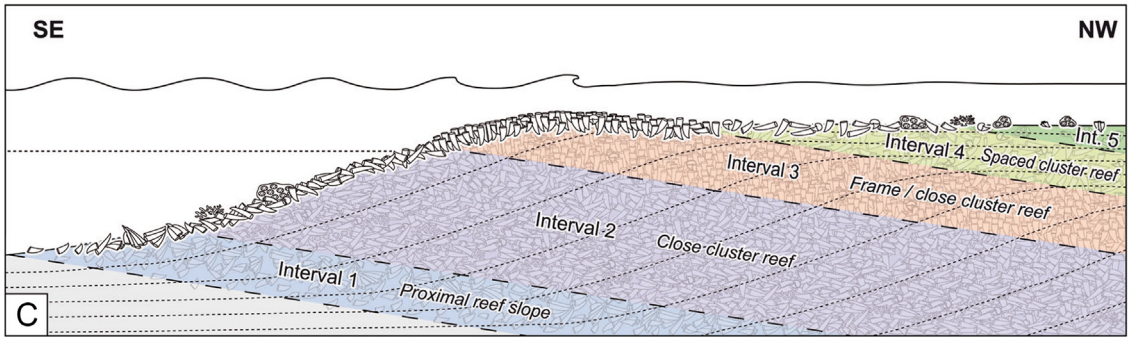
SE
NW
Interval 1
Interval 2
Interval 3
Interval 4
Int. 5
Proximal reef slope
Close cluster reef
Frame / close cluster reef
Spaced cluster reef
C

massive corals, bivalves (including rudists), calcareous red algae (mostly branched) and echinoderm fragments, together with pervasively recrystallized, undetermined allochems (see Fig. 3D). Some of these larger skeletal grains present macroborings. The rest of the skeletal assemblage comprises common bivalve fragments, ostracods, red and green algae fragments, and bryozoans, as well as minor gastropod fragments and a scarce presence of benthic foraminifera (simple miliolids, meandropsinids, rotaliids).

Microfacies at the top of interval 4 display a floatstone texture with a packstone matrix. The largest, skeletal allochems are calcareous red algae (encrusting corallinaceans and peyssonnelaceans), and coral and bivalve fragments. Macroborings are present on the rudist fragments, while red algae are encrusting their surface (see Fig. 3E). Bivalve and coral fragments show surface micritization related to microboring organisms (possible microbial origin). Most of the allochems in the matrix have been dissolved and the molds occluded with calcite cement, which makes them difficult to identify. The rest comprises common bivalve fragments, minor echinoid fragments, and rare green algae and ostracods.

This interval is the most diverse, being the only one containing tall five rudists from the site: a few *Mitrocaprina* sp., very rare *Hippuritella lapeirousei* (only present in the uppermost part), common *Hippuritella* sp., common *Hippurites radiosus,* and rare radiolitids.

4.5. Interval 5

This interval, at the top of the studied section, is 6 m thick and does not contain large rudist shells. Therefore, no orientations were taken.

Interval 5 microfacies show an upwards increase in micritic matrix, fine-grained quartz and glauconite grains, and an overall reduction in allochem size. Microfacies show slight variations throughout the interval. Thus, the base of the interval is a floatstone with an abundant wacke-packstone micritic matrix. The largest allochems are coral (affected by dissolution) and bivalve fragments (including rudists), and calcareous red algae (some coating larger skeletal grains). The fossil fauna in the matrix is fine-grained, and most of them are affected by recrystallization. Common bivalve fragments, minor bryozoan and echinoderm fragments, serpulids, and ostracods, together with very rare benthic foraminifera (miliolids and small meandropsinids) are present.

The middle part shows a packstone texture with a recrystallized micritic matrix. Although a large number of the allochems are recrystallized, it has been possible to identify common bivalve, echinoid, and bryozoan fragments, and a minor presence of coral fragments and benthic foraminifera (miliolids, rotaliids).

At the top, the main texture is a wackestone (see Fig. 3E), with the micritic matrix and skeletal allochems partially replaced by very fine to cryptocrystalline dolomite. Some of the skeletal allochems are still identifiable: bivalve (including rudists), bryozoan and echinoid fragments, and a scarce presence of benthic foraminifera (small meandropsinids and miliolids).

This is the interval with fewer rudists, with very rare *Mitrocaprina* sp., few *Hippuritella lapeirousei* very rare *Hippuritella* sp., very rare radiolitids, and a lack of *Hippurites radiosus*.

In addition to the outcrop studied in detail, isolated outcrops can be found until 600 m away from the studied main outcrop, a W-NW continuous lateral extension of 200 m is observed for intervals 2 and 3. Through such distance the outcrops display the same macroscopic features (see Fig. 2C, D and E) as in the main (road-cut) outcrop. Farther than these distances the reef can be hardly observed among vegetation, except for a limited outcrop found at a mountain road (see upper right in Fig. 1D), where *H. radiosus* is also observed in deposits similar to those of intervals 2 and 3.

5. Discussion

According to the proportions and relationships between the matrix and the rudist shells, and microfacies observations, each interval in the l'Espà reef can be correlated with a depositional setting (see Fig. 5B). Such correlation is supported by the large consistency observed between the five descriptive units and the distinctive way in which rudists are oriented within these units. This vertical succession of environments depicts a complete rudist reef progradation (see Fig. 5B) that could be applied to most reefs. As pointed out by Riding (2002), the classic classification of reefs according to the dominant organism (coral reef, rudist reef, etc.) is unambiguous, but fails to recognize the common features that most reefs share despite the building organism. The structural classification by this author is straightforwardly correlated with interval 2 to 5 from the l'Espà reef. In that way, recordedreef structures are: 'Close cluster reef' (interval 2), 'Frame/Close cluster reef' (interval 3), 'Spaced cluster reef' (interval 4) and 'Very spaced cluster reef' (interval 5) (see Fig. Suppl. 3).

Interval 1 is here interpreted to be the most distal setting: a proximal reef slope. A combination of two processes can be inferred: (1) low energy conditions represented by marl deposition and (2) gravity displacement of unaltered rudists (well-preserved connected valves). The large rudist bunches of grouped specimens (see Fig. 2A and B) indicate that once deposited, they underwent no reworking. The original, random depositional orientation was thus preserved. This would be the result of deposition in a relatively deeper setting, where no wave reworking took place. Such a deeper setting would also be supported by the limited endo-epibiont evidence, being the same observed in the life position rudists of interval 3.

In contrast, interval 2 displays important endo and epibiont colonization, and relative shallow (photic) conditions for large corals to grow. Rudists are more disarticulated than in interval 1 and tend to be flat-lying and in contact with one another. It correlates with a close cluster reef in the sense of Riding (2002), and would represent the halfway between the distal and proximal setting.

Interval 3 is the proximal reef setting, with specimens tending to be vertical and clustered (Fig. 2D, E and F) in bunches of in situ congregations. This skeletal growth permits matrix stabilization by trapping sediment. The structure of this interval resembles those rigid structures described in the Campanian of Oman by Schuman (1995).

The spaced cluster reef of interval 4 displays the coarsest grain sizes and it is represented as the most energetic setting. This is also evidenced by the abundant presence of 'encrusting' algae on the larger rudists fragments. Few specimens are found, most of them highly reworked and sparse within a matrix. This unit likely records the reworking due to wave action at the proximal back reef setting. The texture of the upper part of interval 4 (wackestone with micritic matrix and skeletal allochems) is a transition towards interval 5.

Fig. 5. A: Cartesian 2D plot of inclination of *Hippurites radiosus* at the l'Espà reef. Inclination angles are located in the corresponding stratigraphic height. Note the larger dispersion in intervals 1 and 2 (with even revered specimens) and the grouping in interval 3 (in situ, specimens in a live position). See also the transition between 2 and 3 intervals. Interval 4 dispersion resembles that of interval 2. To the right: distribution of rudists, corals, and endo-epibiont colonization. Qualitative occurrence ranges from abundant (thicker line), common (medium/thick line), few (medium/thin line), rare (thin line) and very rare (dashed thin line). B: Model of reef zonation according to the observed vertical succession and hippuritids orientation. C: Model of the reef zonation according to the defined intervals.

Interval 5, with few fragments of small rudists, is interpreted as a back-reef depositional setting, being dominated by low energy conditions (restricted back-reef).

As a general observation, reworking is a very important process in reef building, since the frame reef (interval 3, proximal reef setting) is just a minor part of the whole reef (10% of the succession). This is the only part where no reworked specimens at all are found (with not a single reverse specimen) and where orientations are rather clustered and with relatively high values of inclination. In fact, a general short life span has been attributed to rudists (from 3 to 11 years), providing high-performance carbonate factories despite the common mechanical breakdown and

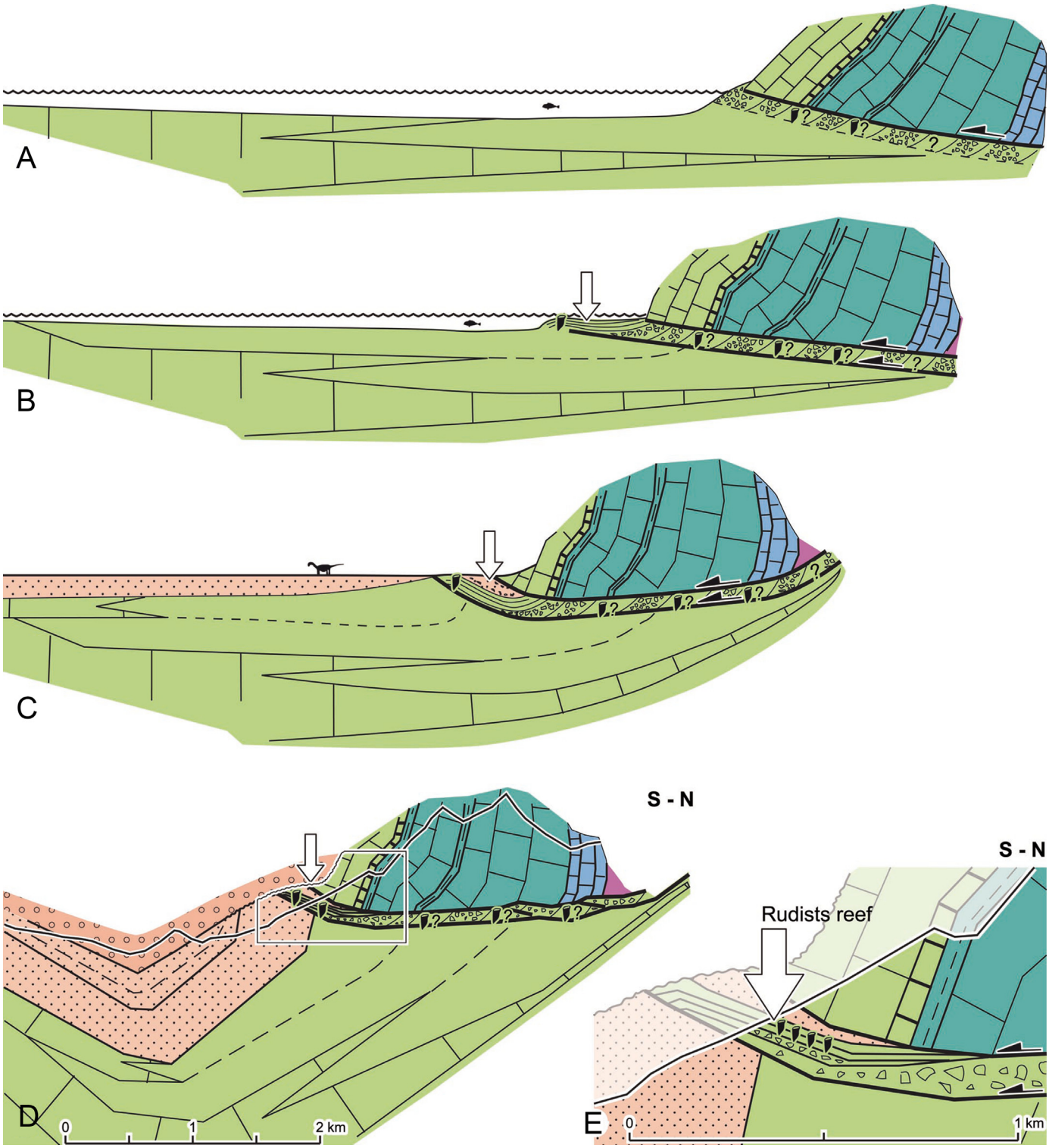

Fig. 6. Synsedimentary evolution sketch of the Intermediate Unit of the Pedraforca thrust sheet. A: Sedimentation of the marine succession previous to the reef-building; B: Reef growth (white arrow); C: Sedimentation of the terrestrial Tremp formation; D: Present-day outcrops with polygon indicating Fig. 6E; E: Detailed cross-section of present-day outcrops. See Fig. 1 for the legend.

bioerosion (Sanders, 1998; Steuber, 2000). Interestingly, if the orientations above and below the in situ reef (interval 3) are compared, a similar dispersion is observed. That is to say, both seaward and landward of the frame reef, orientations alone are not diagnostic of the depositional setting and need to be coupled with facies and microfacies analysis. In any case, large gravity-reworked articulated and unaltered bouquets are only found seawards of the frame reef, indicating a more significant deepening gradient seawards than landwards. This suggests the occurrence of a barrier reef, a structure that can be observed in the 'Homes Morts' locality in the same basin (see Fig. 1 and Fig. Suppl. 4b and 4d). The occurrence of a prograding barrier would require high carbonate productivity, which has been documented to be variable in Late Cretaceous rudists (Steuber, 1996; Steuber et al., 1998). These last studies describe annual vertical growths of 45 mm for the cluster elevator *Vaccinites ultimus*, which is comparable to *Hippurites radiosus* from L'Espà. Thus, the l'Espà reef is considered to have been of high growth rate and high carbonate production. A carbonate production exceeding the creation of accommodation space would permit the reef to prograde. The reef is preserved because there was sufficient subsidence and it was successively drowned. Obviously, the studied reef was formed over several hundreds or thousands of years. On the other hand, thrust progression takes place at a longer scale (higher than thousands of years) but is a stepwise process. This is evidenced by the occurrence of other *H. radiosus* reefs in the Pedraforca Intermediate Unit (see Fig. Suppl. 4c).

The occurrence of a reef crest would be in conflict with the structure of other known hippuritid reefs (Gili et al., 1995; Vilardell and Gili, 2003; Gil et al., 2009), where in situ specimens occurred as bafflers forming bafflestones. In our study case, we observe that the reef had a rigid framework, at least in interval 3. Interestingly, the l'Espà reef has different features when compared to the referred study cases. The mentioned examples refer to relatively small species, all of them being smaller than 3 cm in diameter, while the dominant *H. radiosus* at l'Espà is larger (see before), being more resistant to high energy systems. Similarly, the elongated (right) valves of *H. radiosus* may exceed values of 70 cm, while in the other cases they are generally shorter than 40 cm. Second, l'Espà has a low diversity of hippuritid species, being only 3 (1 *Hippurites* and 2 *Hippuritella*), while in the case of Vilanoveta (Vicens et al., 1998) it is up to 12 (5 *Hippurites*, 5 *Vaccinites*, and 2 *Hippuritella*), while in Castrojimeno is only of 2 (*Hippurites* and *Vaccinites*, Gil et al., 2009), but radiolitids are important reef builders in this last case. Finally, the matrix in tight frames with large rudists, such as the one found in the l'Espà reef or those described in Central Oman by Schumann (1995), reflects a relatively energetic depositional setting, since a muddy substrate would not enhance the stability of such heavy and cluster elevators (see Mitchell 2002). Rudist elevators growing in muddy substrates are isolated forms (such as in Masse and Fenerci-Masse, 2008) and not cluster elevators such as *Hippurites radiosus* from l'Espà.Several works identify cluster elevator rudists as formers of prograding reef barriers. The work by Bialik et al. (2021) reports elevator forms as prograding reefs in the Cenomanian of Israel. Malak and Al-Banna (2014) describe *Durania* (a large radiolitid elevator from the Late Cretaceous of Iran) as barrier-forming in coincidence with reduced diversity, as in our study case (see interval 3 in Fig. 5). Afghah (2021) also describes rudists reefs associated to barriers. Bian et al. (2022) describe rudists frameworks building up reefs at the shelf margin in the Cenomanian of the United Arab Emirates. Other studies such as Khoshnoodkia et al. (2022) describe a basin in the Albian to Santonian from Iran where rudists reefs grow both in shelves and ramps. Thus, l'Espà reef better matches a model of varying energy conditions forcing reef progradation rather than being a strictly ecological succession.

The similarities between coral reefs and our study are relative since it has to be considered that the large species of clustered elevator rudist would largely be influenced by the environmental conditions, i.e., in relatively energetic settings long elevators would grow, whereas in lower energy conditions (lagoon) small specimens are found (see also Fig. 5). On the contrary, coral reefs are also influenced by the energy of the environment in a different way: larger corals do not grow in areas with high energy conditions (Hubbard and Dullo, 2016). Additionally, the thickness of in situ parts of the reef is smaller in rudists (2.5 m in the studied case; see Fig. Suppl. 4a, b) than in coral reefs.

The information so far gathered from the l'Espà reef succession can also contribute to the regional understanding of the synorogenic paleogeographic evolution of the Upper Pedraforca thrust emplacement. The paleogeographic role of the Upper Pedraforca thrust in the formation of the Intermediate Unit is obvious after the occurrence of the marine breccia that was directly sourced from the paleomassif. The prograding succession of the l'Espà reef, together with the orientation of its rudists, provides additional paleogeographic information. From one side, the occurrence of a back reef (interval 4) and the distal back reef settings (interval 5), indicates that the l'Espà reef was not directly rimming a paleorelief (see Fig. 6). This paleorelief could be the Upper Pedraforca paleomassif or another relief located southwards. From the other side, the seaward plunging of rudists towards NW (as seen in interval 3), indicates that this was also the direction of progradation, showing that proximal reef areas were located closer to the inland (ancient Pedraforca massif), and that the open sea was located in the direction of progradation. In the stated model, the reef would be the result of a shallowing induced by the progression of the Upper Pedraforca thrust and would not match those cases where sequence stratigraphy rules rudist reef development (such as in Mülayim et al., 2020).

6. Conclusions

The l'Espà reef displays a vertical succession of the following reefs structures: 'Proximal reef slope' (Distal reef setting), 'Close cluster reef' (Halfway distal to proximal reef), 'Frame/Close cluster reef' (Proximal reef), 'Spaced cluster reef' (proximal back reef) and 'Very spaced cluster reef' (Distal back reef).

This reef succession is supported by microfacies analysis. Interval 1 microfacies are the most distal and the muddiest, while interval 2 microfacies are halfway from the distal and proximal settings. Interval 3 microfacies are consistent with an entirely in situ reef, while interval 4 microfacies (coarser and larger grain sizes) represent the most energetic setting with reef reworking. Interval 5 shows characteristics of a low-energy, restricted, back reef setting.

This complete succession defines a robust model for the original reef structure of *Hippurites radiosus*, that would be the result of a shallowing induced by the progression of the Upper Pedraforca thrust emplacement, Sediment production and accumulation then outpaced relative sea-level rise so that the reef structure prograded. The common appearance of ex-situ specimens of this species throughout the Pyrenees suggests that the structure of the original reef crests had limited potential for preservation because it was relatively thin (maximum preserved thickness is 2.5 m) and was easily eroded by mechanical breakdown and bioerosion.

A clear relationship is observed between reef structure and the occurrence of endo-epibionts, being better typical of the close cluster reef.

The orientation of the in-situ shells (frame/close cluster reef) displays specimens leaning towards the north/northwest,

indicating the paleoslope during reef formation and thus improving the paleogeographic scheme.

The obtained hippuritid reef model has a strong similarity with most coral reefs. Although general models in the literature exclude the presence of a barrier and a back reef environment, in the l'Espà reef it seems to be the most feasible interpretation.

Data availability

The dataset is now included as supplementary material (Tab. suppl. 1)

Acknowledgments

This study is part of the research of project PGC2018-101575-B-I00 'Dynamics of transitional environments from Cretaceous to Eocene in the South-central Pyrenees (PALEOTRANS)' by Ministerio de Ciencia, Innovación y Universidades. E.V. and O.O. belong to the research group '2017 SGR 1666 GRC'. The advice by Josep Maria Pons (Universitat Autònoma de Barcelona) in this study is highly appreciated. Lluís Ardèvol kindly provided the image of Fig. Suppl. 4c. Individual contribution: all authors did fieldwork, EV and OO did the conceptualization, CB did the microfacies study, OO wrote the paper and did project administration, and VR prepared stereoplots. This study has been largely improved after the comments by Prof. Dr. Sacit Özer and an anonymous reviewer. Oriol Oms reports financial support was provided by Ministerio de Ciencia, Innovación y Universidades.

References

Afghah, M., 2021. Microfacies and depositional environment of Tabur Formation (Upper Cretaceous – Lower Paleocene) Zagros area, southwestern Iran. Geological Journal 57, 2868–2883. https://doi.org/10.1002/gj.4450.

Allmendinger, R.W., Cardozo, N., Fisher, D., 2012. Structural geology algorithms: Vectors and tensors in structural geology. Cambridge University Press, p. 289.

Bian, C., Yang, T., Zhang, Q., Lv, M., Li, Y., Liu, G., Duan, H., Luo, B., Zhang, X., Huang, Q., Yang, P., Shi, S., Zhang, J., 2022. Sedimentology, sequence stratigraphy and their control on reservoirs quality in mid-Cretaceous Mishrif formation in East Rub al Khali Basin, Western UAE. Carbonates and Evaporites 37, 71. https://doi.org/10.1007/s13146-022-00814-0.

Bialik, O.M., Samankassou, E., Meilijson, A., Waldmann, N., Steinberg, J., Karcz, K., Makovsky, Y., 2021. Short-lived early Cenomanian volcanic atolls at Mt. Carmel, northern Israel. Sedimentary Geology 411, 105805. https://doi.org/10.1016/j.sedgeo.2020.105805.

Bilotte, M., 1985. Le Crétacé supérieur des plates-formes est-pyrénéenes. Strata, Série 2, Mémoires, vol. 5, p. 485. Toulouse.

Bosence, D., 2005. A genetic classification of carbonate platforms based on their basinal and tectonic settings in the Cenozoic. Sedimentary Geology 175, 49–72. https://doi.org/10.1016/j.sedgeo.2004.12.030.

Caus, E., Frijia, G., Parente, M., Robles-Salcedo, R., Villalonga, R., 2016. Constraining the age of the last marine sediments in the late Cretaceous of central south Pyrenees (NE Spain): Insights from larger benthic foraminifera and strontium isotope stratigraphy. Cretaceous Research 57, 402–413. https://doi.org/10.1016/j.cretres/2015.05.012.

García Senz, J., 2002. Cuencas extensivas del Cretácico inferior en los Pirineos Centrales, formación y subsecuente inversión (PhD thesis). Universitat de Barcelona. Departament de Geodinàmica i Geofísica, p. 310. https://www.tdx.cat/handle/10803/1913#page=1.

Gil, J., Pons, J.M., Segura, M., 2009. Succession of rudistid lithosomes along the western coastal margin of the Iberian Basin (Coniacian, Castrojimeno Section, central Spain). Facies 55, 523–538. https://doi.org/10.1007/s10347-009-0186-4.

Gili, E., Skelton, P.W., Vicens, E., Obrador, A., 1995. Corals to rudists – an environmentally induced assemblage succession. Palaeogeography, Palaeoclimatology, Palaeoecology 119 (1–2), 127–136. https://doi.org/10.1016/0031-0182(95)00064-X.

Götz, S., 2003. Biotic interaction and synecology in a Late Cretaceous coral-rudist biostrome of southeastern Spain. Palaeogeography, Palaeoclimatology, Palaeoecology 193, 125–138. https://doi.org/10.1016/S0031-0182(02)00719-8.

Hubbard, D.K., Dullo, W.-C., 2016. The changing face of reef building. In: Hubbard, D.K., et al. (Eds.), Coral Reefs of the World, vol. 6, pp. 127–154. https://doi.org/10.1007/978-94-017-7567-0.

Khoshnoodkia, M., Rahmani, O., Adabi, M.H., Hosseini-Barzi, M., Mahdi, T.A., 2022. Depositional environment, seismic stratigraphy, and Sr-isotope geochronology, Bangestan reservoir, Ahwaz oilfield, SW Iran. Journal of Petroleum Science and Engineering 208 (2022), 109629. https://doi.org/10.1016/j.petrol.2021.109629.

Malak, Z.A., Al-Banna, N.Y., 2014. Sequence stratigraphy of Aqra Formation (Late Upper Campanian–Maastrichtian) in Geli Zanta corge, Northern Iraq. Arabian Journal of Geosciences 7, 971–985. https://doi.org/10.1007/s12517-012-0822-0.

Martínez, A., 2000. L'Espà-Saldes. In: Inventari d'Espais d'Interès Geologic de catalunya, vol. 146. Generalitat de Catalunya. http://mediambient.gencat.net.

Martínez, A., Berástegui, X., Losantos, M., Schöllhorn, E., 2001. Estructura de los mantos superior e inferior del Pedraforca (Pirineos orientales). Geogaceta 30, 183–186. https://sge.usal.es/archivos/geogacetas/Geo30/Art46.pdf.

Masse, J.-P., Fenerci-Masse, M., 2008. Time contrasting palaeobiogeographies among Hauterivian–Lower Aptian rudist bivalves from the Mediterranean Tethys, their climatic control and palaeoecological implications. Palaeogeography, Palaeoclimatology, Palaeoecology 269, 54–65. https://doi.org/10.1016/j.palaeo.2008.07.024.

Mitchell, S.F., 2002. Palaeoecology of corals and rudists in mixed volcaniclastic-carbonate small-scale rhythms (Upper Cretaceous, Jamaica). Palaeogeography, Palaeoclimatology, Palaeoecology 186, 237–259.

Moeri, E., 1977. Oberkretazische Schelfsedimente in der Zentralpyrenaen zwischen Río Segre und Llobregat. Eclogae Geologicae Helvetiae 70 (1), 193–235. https://www.e-periodica.ch/digbib/volumes?UID=egh-001.

Mülayim, O., Yilmaz, I.Ö., Özer, S., Bilal Sarı, B., Taslı, K., 2020. A Cenomanian-Santonian rudist-bearing carbonate platform on the northern Arabian Plate, Turkey: facies and sequence stratigraphy. Cretaceous Research 110. https://doi.org/10.1016/j.cretres.2020.104414.

Muñoz, J.A., Mencos, J., Roca, E., Carrera, N., Gratacós, O., Ferrer, O., Fernández, O., 2018. The structure of the South-Central-Pyrenean fold and thrust belt as constrained by subsurface data. Geológica Acta 16 (4), 439–460. https://doi.org/10.1344/GeologicaActa2018.16.4.7.

Negra, M.H., Skelton, P.W., Gili, E., Valldeperas, F.X., Argles, T., 2016. Recognition of massive Upper Cretaceous carbonate bodies as olistoliths using rudist bivalves as internal bedding indicators (Campanian Merfeg Formation, Central Tunisia). Cretaceous Research 66, 177–193. https://doi.org/10.1016/j.cretres.2016.06.003.

Oms, O., Dinarès-Turell, J., Vicens, E., Estrada, R., Vila, B., Galobart, À., Bravo, A.M., 2007. Integrated stratigraphy from the Vallcebre section (Southeastern Pyrenees, Spain): New insights on the continental Cretaceous–Tertiary transition in southwest Europe. Palaeogeography, Palaeoclimatology, Palaeoecology 255, 35–47. https://doi.org/10.1016/j.palaeo.2007.02.039.

Oms, O., Fondevilla, V., Riera, V., Marmi, J., Vicens, E., Estrada, R., Anadón, P., Vila, B., Galobart, À., 2016. Transitional environments of the lower Maastrichtian South-Pyrenean Basin (Catalonia, Spain): the Fumanya Member tidal flat. Cretaceous Research 57, 428–442. https://doi.org/10.1016/j.cretres.2015.09.004.

Özer, S., Benyoucef, M., 2021. Late Cenomanian rudists from southern Algeria: descriptions, biostratigraphy, palaeoecology and palaeobiogeography. Cretaceous Research 118. https://doi.org/10.1016/j.cretres.2020.104639.

Riding, R., 2002. Structure and composition of organic reefs and carbonate mud mounds: concepts and categories. Earth-Science Reviews 58, 163–231. https://doi.org/10.1016/S0012-8252(01)00089-7.

Robles-Salcedo, R., Rivas, G., Vicedo, V., Caus, E., 2013. Paleoenvironmental distribution of larger foraminifera in Upper Cretaceous siliciclastic – carbonate deposits (Arén sandstone formation, South Pyrenees, Northeastern Spain). PALAIOS 28 (9), 637–648. https://www.jstor.org/stable/43683739.

Robles-Salcedo, R., Vicedo, V., Caus, E., 2018. Latest Campanian and Maastrichtian Siderolitidae (larger benthic foraminifera) from the Pyrenees (S France and NE Spain). Cretaceous Research 81, 64–85. https://doi.org/10.1016/J.CRETRES.2017.08.017.

Sadooni, F.N., 2005. The nature and origin of Upper Cretaceous basin-margin rudist buildups of the Mesopotamian Basin, southern Iraq, with consideration of possible hydrocarbon stratigraphic entrapment. Cretaceous Research 26, 213–224. https://doi.org/10.1016/j.cretres.2004.11.016.

Sanders, D., 1998. Upper Cretaceous 'Rudists formations'. Geologisch-Paläontologische Mitteilungen Innsbruck 23, 37–59. https://www2.uibk.ac.at/downloads/c715/gpm_23/23_037-059.pdf.

Sanders, D., Pons, J.M., 2001. Stratigraphic Architecture of a Santonian Mixed Siliciclastic-Carbonate Succession (Catalonian Pyrenees, Spain). Facies 44, 105–136. https://doi.org/10.1007/BF02668170.

Schumann, D., 1995. Upper Cretaceous rudists and stromatoporoid associations of Central Oman (Arabian Peninsula). Facies 32, 180–202. https://doi.org/10.1007/BF02536868.

Skelton, P., Gili, E., 1991. Paleoecological classification of rudist morphotypes. In: Sladiç-Trifunoviç, M. (Ed.), Proceedings of the first international conference on rudists, vol. 2. Serbian Geol. Soc., Spec. Publ, Beograd.

Skelton, P., Gili, E., Vicens, E., Obrador, A., 1995. The growth fabric of gregarious rudist elevators (hippuritids) in a Santonian carbonate platform in the southern Central Pyrenees Palaeogeography. Palaeoclimatology, Palaeoecology 119, 107–126. https://doi.org/10.1016/0031-0182(95)00063-1.

Steuber, T., 1996. Stable isotope sclerochronology of rudist bivalves: Growth rates and Late Cretaceous seasonality. Geology 24 (4), 315–318. https://doi.org/10.1130/0091-7613(1996)024<0315:SISORB>2.3.CO;2.

Steuber, T., 2000. Skeletal growth rates of Upper Cretaceous rudist bivalves: implications for carbonate production and organism-environment feedbacks. Geological Society, London, Special Publications 178, 21–32. https://doi.org/10.1144/GSL.SP.2000.178.01.03.

Steuber, T., Yilmaz, C., Loser, H., 1998. Growth of Early Campanian rudists in siliciclastic-calcareous setting (Pontids Mts., north-central Turkey). Geobios 31 (1), 385–401. https://doi.org/10.1016/S0016-6995(98)80088-0.

Vergés, A., Martinez, A., 1988. Corte compensado del Pirineo oriental: Geometría de las cuencas de antepaís y edades de emplazamiento de los mantos e corrimiento. Acta Geológica Hispánica 23 (2), 95–105. https://revistes.ub.edu/index.php/ActaGeologica/article/view/4411/5512.

Vicens, E., 1992. Estudio de la fauna de rudistas (Hippuritidae y Radiolitidae) de los materiales cretácicos del Pirineo oriental: implicaciones bioestratigráficas (PhD Thesis). Universitat Autònoma de Barcelona, p. 270.

Vicens, E., López, G., Obrador, A., 1998. Facies succession, biostratigraphy and rudist faunas of Coniacian to Santonian platform deposits in the Sant Corneli anticline (Southern Pyrenees). Geobios 22, 403–427. https://doi.org/10.1016/S0016-6995(98)80089-2.

Vicens, E., Ardèvol, L., López-Martínez, N., Arribas, E., 2004. Rudist biostratigraphy in the Campanian–Maastrichtian at the south-central Pyrenees, Spain. Courier Forschungsinstitut Senckenberg 247, 113–127. https://www.ucm.es/data/cont/media/www/pag-33428/Rudist%20Biostratigraphy.pdf.

Vicens, E., Pons, J.M., Oms, O., Riera, V., 2011. El arrecife de hipurítidos de L'Espà (Campaniense, Pirineos). In: La Transición Cretácico-Terciario en el Sur de los Pirineos, 6Paleontologia i Evolució Special Memoir, pp. 35–36. Stop 3, Field Guidebook XXVII Jornadas de la Sociedad Española de Paleontología. Sabadell (Spain) 5–8th October.

Vicens, E., Pons, J.M., Oms, O., 2014. Upper Cretaceous rudists from the Berguedà. Pre-congress field trip. In: 10th International Congress on rudist bivalves. Bellaterra, June 22-27, p. 12 (Unpublished).

Vila, B., Riera, V., Bravo, A.M., Oms, O., Vicens, E., Estrada, R., Galobart, À., 2011. The chronology of dinosaur oospecies in South-Western Europe: refinements from the Maastrichtian succession of the eastern Pyrenees. Cretaceous Research 32 (3), 378–386. https://doi.org/10.1016/j.cretres.2011.01.009.

Vilardell, O., Gili, E., 2003. Quantitative study of a hippuritid rudist lithosome in a Santonian carbonate platform in the southern Central Pyrenees. Palaeogeography, Palaeoclimatology, Palaeoecology 200 (1–4), 31–41. https://doi.org/10.1016/S0031-0182(03)00443-7.

Yamanaka, M., Sano, S., Zaabi, H.B.A., Fujioka, H., Iryu, Y., 2020. Visualization of the morphology and mode of occurrence of Cenomanian rudists within a drillcore by X-ray CT scanning and 3D modeling. Progress in Earth and Planetary Science 7 (49), 12. https://doi.org/10.1186/s40645-020-00359-7.

Yose, L.A., Ruf, A.S., Strohmenger, C.J., Schuelke, J.S., Gombos, A., Al-Hosani, I., Al-Maskary, S., Bloch, G., Al-Mehairi, Y., Johnson, G., 2006. Three-dimensional characterization of a heterogeneous carbonate reservoir, Lower Cretaceous, Abu Dhabi (United Arab Emirates). In: Harris, P.M., Weber, L.J. (Eds.), Giant hydrocarbon reservoirs of the world: From rocks to reservoir characterization and modeling: AAPG Memoir 88/SEPM Special Publication, pp. 173–212. https://doi.org/10.1306/1215877M882562.

Appendix A. Supplementary data

Supplementary data to this article can be found online at https://doi.org/10.1016/j.cretres.2023.105507.